JOURNAL OF SOLID STATE CHEMISTRY 103, 253–262 (1993)

Structural Phase Transition of $La_4BaCu_5O_y$

MASAKI KATO, NOBUTAKA KOJIMA,[1] KAZUYOSHI YOSHIMURA, YUTAKA UEDA,[2] NORIAKI NAKAYAMA, AND KOJI KOSUGE

Department of Chemistry, Faculty of Science, Kyoto University, Kyoto 606-01, Japan

AND ZENJI HIROI AND YOSHICHIKA BANDO

Institute for Chemical Research, Kyoto University, Uji, Kyoto-fu 611, Japan

Received June 1, 1992; in revised form August 25, 1992; accepted August 26, 1992

By the heat treatment of tetragonal $La_4BaCu_5O_y$ under flowing high-purity N_2 gas followed by slow cooling, we could newly synthesize a single phase of monoclinic $La_4BaCu_5O_y$ which is metallic but nonsuperconducting, as well as the tetragonal $La_4BaCu_5O_y$. From the carbon reduction method and thermogravimetric analysis, we have determined the values of the oxygen content y to be 13.0 and 12.5 for the tetragonal and new monoclinic phases, respectively. Electron diffraction patterns of the monoclinic phase show superlattice reflections corresponding to a $\sqrt{10}a_p \times \sqrt{10}a_p \times a_p$ unit cell. (a_p means the unit dimension of fundamental perovskite structure.) *In-situ* XRD measurements at high temperatures have revealed the following two facts: (1) in air, $La_4BaCu_5O_y$ has a tetragonal structure with a $\sqrt{5}a_p \times \sqrt{5}a_p \times a_p$ unit cell up to 1040°C, accompanying the oxygen loss up to 12.5 with the increase of temperature; and (2) the monoclinic phase, closed in an evacuated quartz capillary, transforms into the tetragonal phase above 690°C.

1. Introduction

Since the discovery of superconductivity with high critical temperature in the layered perovskite copper oxides (*1*), much research has been done on these compounds. As a result it has been established that the CuO_2 layer plays an essential role in the origin of superconductivity. Several oxygen-deficient perovskites, on the other hand, have been studied from the points of view of mixed valence states of copper and also their electric conductivity for their potential applications in catalysis, electrocatalysis, or as gauges (*2*). It is important to investigate the dependence of the structure and the physical properties on the oxygen content in these oxides related to superconductivity. Among those oxides, an oxygen-deficient perovskite $La_4BaCu_5O_y$ ($y \cong 13$) with a complex Cu–O network shows metallic conductivity (*3*, *4*) although it is nonsuperconducting (*5*). Recently, copper nuclear quadrupole or magnetic resonance for CuO_5 sites of $La_4BaCu_5O_y$ has revealed that the behaviors of copper spin fluctuations are different from those in superconducting oxides (*6*).

The crystal structure of $La_4BaCu_5O_{13.0}$,

[1] Present address: Asahi Glass Co., Ltd., Taketoyo-cho, Chita-gun 470-23, Japan.

[2] Present address: Institute for Solid State Physics, The University of Tokyo, Roppongi 7-22-1, Minatoku, Tokyo 106, Japan.

0022-4596/93 $5.00

synthesized in air, was found to be a tetragonal symmetry of $P4/m$ space group, as reported by Michel *et al.* (*4*). We have preliminarily reported the synthesis of a new monoclinic phase of $La_4BaCu_5O_y$, whose oxygen content y is 12.5 less than that of the tetragonal phase (*7*). Davies and Katzan (*8*) also independently investigated the structural change of $La_4BaCu_5O_y$ as a function of the oxygen content and found some new phases with $y \cong 12.5$ (phase I'), 12 (phase II), and 11 (phase III). The phase I' was found to be identical to the monoclinic phase we reported previously.

In this paper, we report the thermal and structural relationship between the tetragonal $La_4BaCu_5O_{13.0}$ and the monoclinic $La_4BaCu_5O_{12.5}$ studied mainly by *in situ* X-ray diffraction measurement up to high temperatures. This newly found monoclinic phase of $La_4BaCu_5O_{12.5}$ shows nonsuperconducting but metallic conductivity, as well as the tetragonal phase of $La_4BaCu_5O_{13.0}$.

2. Experimental

Samples of $La_4BaCu_5O_y$ were prepared by solid-state reactions of La_2O_3, $BaCO_3$, and CuO with 99.99% purity. The raw materials were mixed carefully, pelletized and heated in air at 900°C for 2 days for both decarbonization and provisional reactions. Then, the sample was ground, pelletized, and heated again at 1000°C for 2 days. We obtained $La_4BaCu_5O_y$ samples with tetragonal structure having $a = 8.644$ and $c = 3.856$ Å. The obtained sample was divided into several pieces, each of which was treated by the following sequences of heat treatments: (1) firing at 780°C and cooling slowly at rate of 2°C/min in flowing N_2 gas with high purity of above 99.999%; (2) quenching into liquid N_2 after firing in air at various temperatures. The phase identification was carried out by powder X-ray diffraction (XRD) using Cu$K\alpha$. As a result of these heat treatments we newly obtained monoclinic $La_4BaCu_5O_y$ with $y \cong 12.5$. By XRD at high temperatures (HXRD) we studied the structural relation between the tetragonal and monoclinic phases. HXRD experiments were performed for the tetragonal $La_4BaCu_5O_y$ in air using Cu$K\alpha$ radiation and for the monoclinic $La_4BaCu_5O_y$ in evacuated capillary quartz tubes using Mo$K\alpha$ radiation. Oxygen contents were measured by the carbon reduction method (CRM) using the apparatus, Horiba, EMGA-550, and by thermogravimetric analysis (TGA). Electron diffraction (ED) was performed to elucidate the structural properties. DC resistivity was measured down to 2.6 K using the conventional four-terminal method.

3. Results and Discussion

Figure 1a shows the powder XRD pattern of $La_4BaCu_5O_y$ prepared by firing in air at 1000°C. The crystal structure was found to have tetragonal symmetry with $P4/m$ space group as reported by Michel *et al.* (*4*). First, we investigated the homogeneity range of $La_4BaCu_5O_y$, i.e., $La_{4+\delta}Ba_{1-\delta}Cu_5O_y$. By changing the ratio of cations (La, Ba) from the stoichiometric composition (4 : 1) in a small amount, we could not obtain any single phase. For example, a sample with nominal composition of $La_{4+\delta}Ba_{1-\delta}Cu_5O_y$ was a

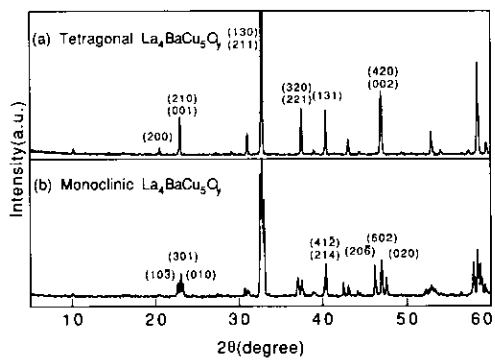

FIG. 1. XRD patterns (a) of tetragonal $La_4BaCu_5O_y$ fired in air at 1000°C, and (b) of monoclinic $La_4BaCu_5O_y$ fired in flowing N_2 gas at 780°C.

three-phase mixture of $La_4BaCu_5O_y$, $La_{2-x}Ba_xCuO_y$, and CuO for $\delta = 0.05$, and was a two-phase mixture of $La_4BaCu_5O_y$ and $La_3Ba_3Cu_6O_y$ for $\delta = -0.05$. Therefore, we conclude that there exists a $La_{4+\delta}Ba_{1-\delta}Cu_5O_y$ phase in a very narrow cation composition region of δ (at least $-0.05 < \delta < 0.05$) around the stoichiometric composition (4 : 1). Second, we performed another sequence of heat treatment. Samples of tetragonal $La_4BaCu_5O_y$ were heated in flowing N_2 gas at 780°C for 2 days followed by cooling slowly in the same atmosphere. A typical XRD pattern of the obtained sample is shown in Fig. 1b. All the peaks in this pattern could be indexed on the basis of monoclinic symmetry with $a = 12.23$ Å, $b = 3.817$ Å, $c = 12.38$ Å, and $\beta = 90.54°$ with only a small modification from the tetragonal phase indices. The obtained XRD data for tetragonal and monoclinic phases are summarized in Table I. Here, tetragonal and monoclinic unit vectors are related to basal perovskite unit vectors as

$$\mathbf{a}_t = 2\mathbf{a}_p - \mathbf{b}_p, \quad \mathbf{b}_t = \mathbf{a}_p + 2\mathbf{b}_p, \quad \mathbf{c}_t = \mathbf{c}_p \quad (1)$$

$$\mathbf{a}_m = 3\mathbf{a}_p + \mathbf{b}_p, \quad \mathbf{b}_m = \mathbf{c}_p, \quad \mathbf{c}_m = \mathbf{a}_p - 3\mathbf{b}_p, \quad (2)$$

where the suffixes "t," "m," and "p" stand for tetragonal, monoclinic, and perovskite units, respectively. We could also synthesize the monoclinic phase by heating in air in the temperature range of 950° ~ 1000°C followed by quenching into liquid N_2. As mentioned below, CRM and TGA experiments shows that the oxygen content y of the monoclinic phase is about 12.5. Two additional oxygen-deficient phases with $y =$ 12 and 11 were reported recently (*8*). These phases could be synthesized at low temperatures under 15% H_2/85% Ar gas. We could not obtain any single phases by firing at higher than 780°C in flowing N_2 gas. We show a typical XRD pattern of a sample decomposed by the heat treatment at 900°C

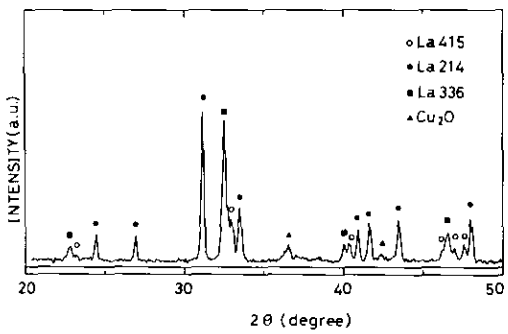

FIG. 2. An XRD pattern indicating the decomposition of $La_4BaCu_5O_y$ by the reduction treatment in flowing N_2 gas at 900°C.

in N_2 gas in Fig. 2. One can find that the sample is decomposed into La_2CuO_4, $La_3Ba_3Cu_6O_y$, and Cu_2O.

From CRM experiments and TGA in flowing 10% H_2/90% He gas, we determine the oxygen composition y of tetragonal $La_4BaCu_5O_y$ fired in air to be 13.0, which agrees well with the value of $y(=13.16)$ reported previously (*4*). Then, we performed TGA measurements in order to investigate the temperature dependence of y both in air and in flowing N_2 gas. As shown in Fig. 3, the decrease of oxygen content y has been observed for both atmospheres with increasing temperature. In flowing N_2 gas, the decrease of y (Δy) amounted to 0.4 at 780°C, and the value of Δy is almost invariable with de-

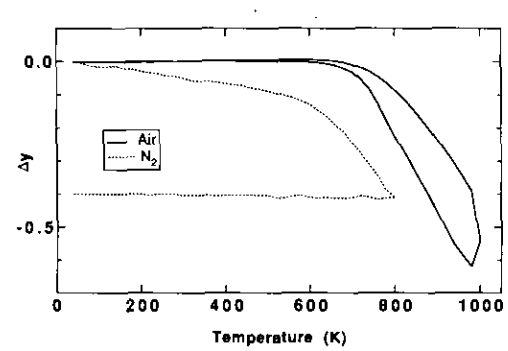

FIG. 3. Temperature dependence of the oxygen content y deduced by TGA.

TABLE I

POWDER XRD DATA OF TETRAGONAL $La_4BaCu_5O_{13.0}$ AND MONOCLINIC $La_4BaCu_5O_{12.5}$

Tetragonal $La_4BaCu_5O_{13.0}$						Monoclinic $La_4BaCu_5O_{12.5}$					
h	k	l	D(cal.)	D(obs.)	I(obs.)	h	k	l	D(cal.)	D(obs.)	I(obs.)
1	0	0	8.644	8.655	2	1	0	$\bar{1}$	8.741	—	—
						1	0	1	8.659	—	—
2	0	0	4.322	4.319	2	2	0	$\bar{2}$	4.371	—	—
						2	0	2	4.330	—	—
2	1	0	3.866	3.864	13	1	0	$\bar{3}$	3.922	3.921	10
						3	0	1	3.860	3.857	17
0	0	1	3.856			0	1	0	3.817	3.811	9
3	0	0	2.881	2.879	7	3	0	$\bar{3}$	2.914	2.910	6
						3	0	3	2.866	2.877	4
2	0	1	2.877								
1	3	0	2.733	2.732	100	4	0	$\bar{2}$	2.751	2.751	88
						2	0	4			
2	1	1	2.730			1	1	$\bar{3}$	2.735	2.731	100
						3	1	1	2.714	2.710	60
3	2	0	2.397	2.397	14	1	0	$\bar{5}$	2.432	2.428	11
						1	0	5	2.423		
						5	0	$\bar{1}$	2.403	2.398	11
						5	0	1	2.395		
2	2	1	2.395			0	1	4	2.404		
						4	1	0	2.386		
						3	1	$\bar{3}$	2.316	2.315	3
						3	1	3	2.302		
1	3	1	2.230	2.229	14	4	1	$\bar{2}$	2.232	2.231	22
						2	1	4			
4	1	0	2.096	2.096	5	3	0	$\bar{5}$	2.125	2.214	10
						5	0	3	2.095	2.096	8
3	2	1	2.036	2.036	1	1	1	$\bar{5}$	2.051	2.046	3
						1	1	5	2.045		
						5	1	$\bar{1}$	2.033	—	—
						5	1	1	2.029	—	—
4	2	0	1.933	1.932	20	2	0	$\bar{6}$	1.961	1.962	23
						6	0	2	1.930	1.931	26
0	0	2	1.928			0	2	0	1.909	1.909	13
5	0	0	1.729	1.728	8					1.748	4
4	2	1	1.728								
2	1	2	1.725							1.727	8
5	1	0	1.695	1.696	1						
3	4	1	1.578	1.578	30					1.590	25
										1.585	11
1	3	2	1.576	1.573	12					1.578	34
										1.569	23
5	1	1	1.552	1.552	4					1.577	9

Note. $La_4BaCu_5O_{13.0}$: a = 8.644 Å and c = 3.856 Å; $La_4BaCu_5O_{12.5}$: a = 12.23 Å, b = 3.817 Å, c = 12.38 Å, and β = 90.54°.

creasing temperature. From TGA experiments of samples kept at 780°C for 1 day, the Δy amounted to a maximum value of 0.5. Hence, the oxygen content y of the monoclinic phase was deduced to be 12.5.

In order to investigate structural properties of these tetragonal and monoclinic phases, we performed ED experiments. For the tetragonal phase, we show a typical ED pattern with the [001] zone axis in Fig. 4a. Note that Miller indices in Fig. 4a are based on the fundamental perovskite unit cell. Consequently, superlattice spots indicate that the tetragonal phase has a unit cell with dimensions of $\sqrt{5}a_p \times \sqrt{5}a_p \times a_p$. In a [001] zone axis ED pattern of the monoclinic phase shown in Fig. 4b, one can find superstructure reflections corresponding to $\sqrt{10}a_p \times \sqrt{10}a_p \times a_p$. Moreover, this ED pattern shows that the fundamental perovskite cell has orthorhombic symmetry (a_p = 3.89 Å, b_p = 3.96 Å). This fact can also be confirmed by XRD measurements as follows. Comparing the XRD pattern of tetragonal phase with that of monoclinic phase in Fig. 1, it is noted that the $(4k\bar{2})$ and $(2k4)$ peaks of the monoclinic phase, which correspond to the $(13l)$ peaks of the tetragonal phase, do not split in contrast to other main peaks. These $(4k\bar{2})$ and $(2k4)$ planes are equivalent to the $(11l)$ and $(1\bar{1}l)$ planes of the fundamental perovskite lattice, respectively. If the angle between a_p- and b_p-axes, γ_p, is not the right angle, spacing of $(11l)$ planes must differ from that of $(1\bar{1}l)$ planes. Thus, the fundamental perovskite cell is distorted to orthorhombic by the heat treatment in flowing N_2 gas. The superstructure observed in the monoclinic phase is considered to be caused by the oxygen deficiency. However, we could not obtain a transmission electron microscope image for the monoclinic phase because of the irradiation damage of electron beams. It will be important to elucidate the location of oxygen vacancies in a unit cell, which is mentioned below.

For the direct observation of phase relation between these phases, HXRD experiments were performed. First, experiments on samples of the tetragonal phase were carried out in air from room temperature up to 1040°C. We show a temperature dependence of lattice parameters in Fig. 5. Note that the observed lattice parameters are converted into those of the fundamental perovskite unit cell ($a_p = a/\sqrt{5}$, $c_p = c$). One can find that the crystal structure has the tetragonal symmetry ($a_p > c_p$) independent of the temperature, although the result of TGA in Fig. 3 shows the oxygen-deficient phase at high temperatures. Second, we did HXRD measurements for samples of the monoclinic $La_4BaCu_5O_y$ which were enclosed in evacuated capillary tubes. Typical XRD patterns at three temperatures are shown in Fig. 6 and the values of lattice parameters are plotted against temperature in Fig. 7. The XRD pattern at room temperature in Fig. 6a shows three pairs of diffraction peaks which correspond to $(20\bar{6})$, (602), and (002) reflections. Since these three peaks are equivalent to (020), (200), and (002) peaks of the fundamental perovskite subcell, they are adequate for the direct observation of the symmetry of the perovskite lattice. At 671°C, the (020) and (200) peaks begin to overlap each other as seen in Fig. 6b and at 694°C it is impossible to distinguish one from the other, as seen in Fig. 6c. We also confirmed that this peak also splits into two peaks reversibly with decreasing temperature again. Thus, when the oxygen content y is fixed at almost 12.5, the crystal structure of $La_4BaCu_5O_y$ is transformed into tetragonal from monoclinic at 690°C. In addition, the symmetry of the fundamental perovskite turn from orthorhombic to tetragonal. The structural transition at 690°C may be of first order but very close to second order, as seen in Fig. 7. It is noted that the lattice parameters, a_p and c_p, of this tetragonal phase around at 700°C are nearly equal to those of the tetragonal phase in

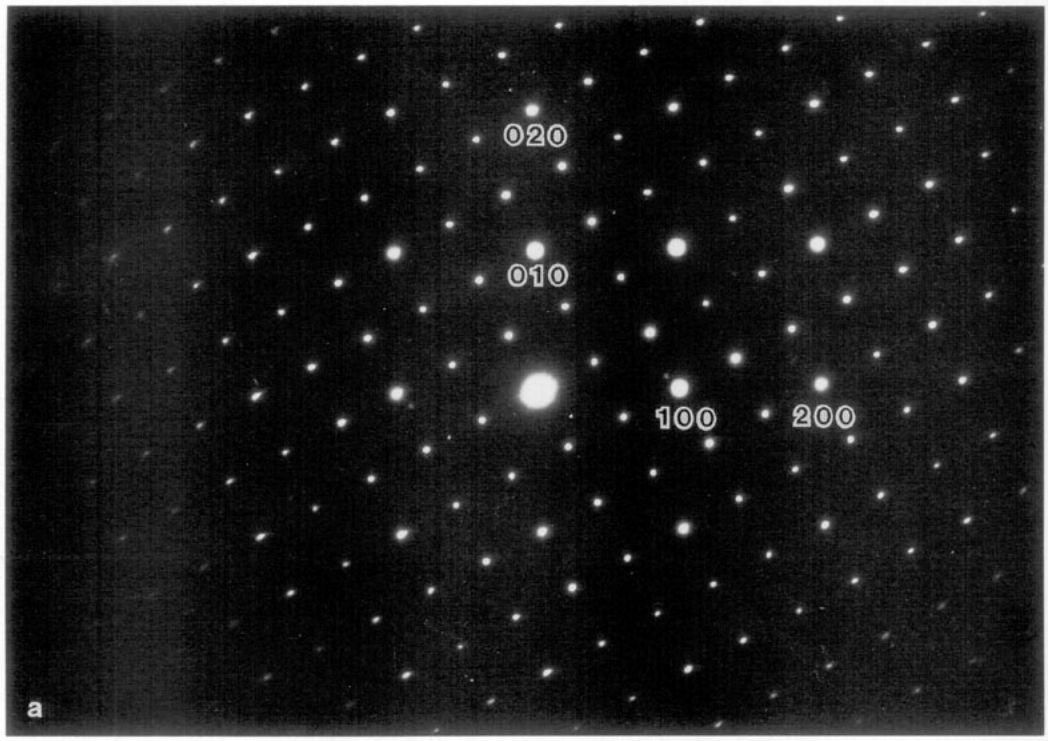

FIG. 4. [001] Zone electron diffraction patterns for (a) the tetragonal phase and (b) the monoclinic phase. Miller indices in the figure are defined by the fundamental perovskite vectors which are related to the tetragonal and monoclinic unit vectors by Eqs. (1) and (2).

air. We can conclude, therefore, that above 690°C $La_4BaCu_5O_y$ is in the single tetragonal phase independent of the oxygen content ($12.5 < y < 13.0$).

Furthermore, we have roughly investigated the phase diagram of $La_4BaCu_5O_y$ as a function of the oxygen content y between 12.5 and 13.0 by means of XRD measurement with samples quenched into liquid N_2 after heating in air at various temperatures. In Fig. 8, we show typical XRD patterns of compounds which are quenched from 850 ~ 1000°C. The HXRD measured *in situ* in air atmosphere indicates that $La_4BaCu_5O_y$ is in a single phase with tetragonal symmetry in this range of temperatures. However, XRD patterns of the samples quenched from 875 and 950°C indicate the coexistence of the tetragonal and monoclinic phases. Hence, we concluded that in the range of $12.5 < y < 13.0$ there exists a two-phase region of monoclinic and tetragonal $La_4BaCu_5O_y$ at low temperatures. The tentative phase diagram can be obtained as shown in Fig. 9. In this figure, the dashed line shows the temperature dependence of the oxygen content in air obtained by TGA experiments.

Michel *et al.* (*4*) proposed a structural model for this phase, as shown in Fig. 10, in which open circle, large solid circle, and small solid circle represent La, Ba, and Cu, respectively. This model structure with $P4/m$ symmetry was confirmed by neutron powder diffraction. As the result of our HXRD experiments, there is a typical feature concerning the site of removed oxy-

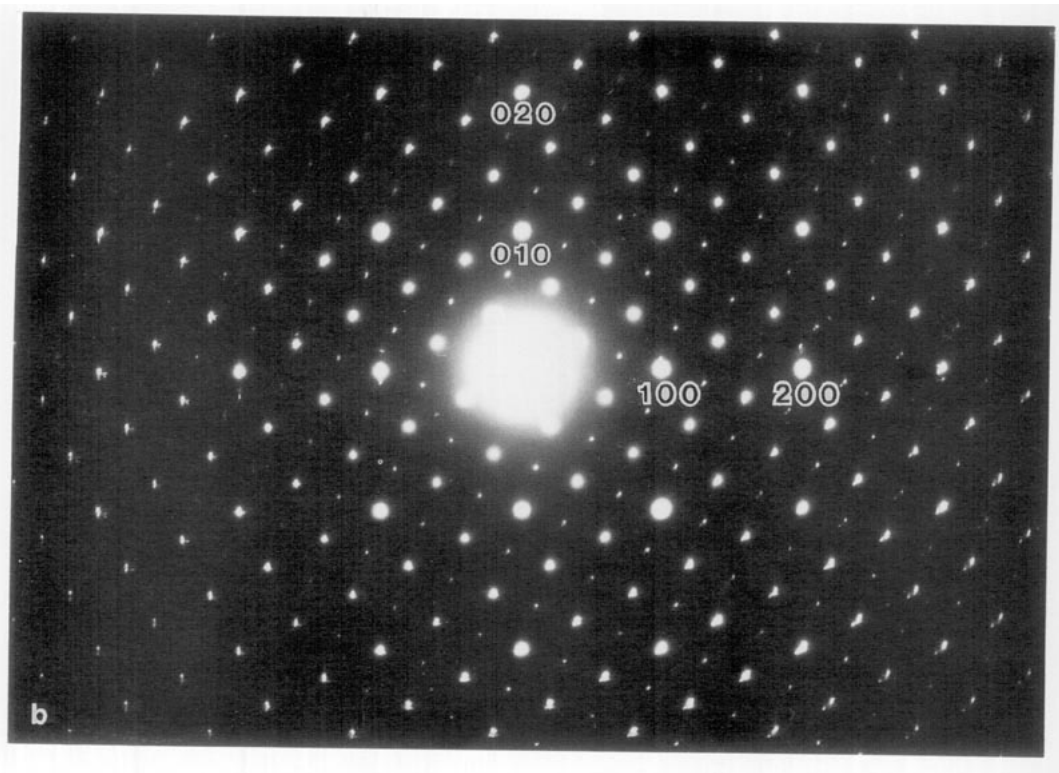

FIG. 4—*Continued*

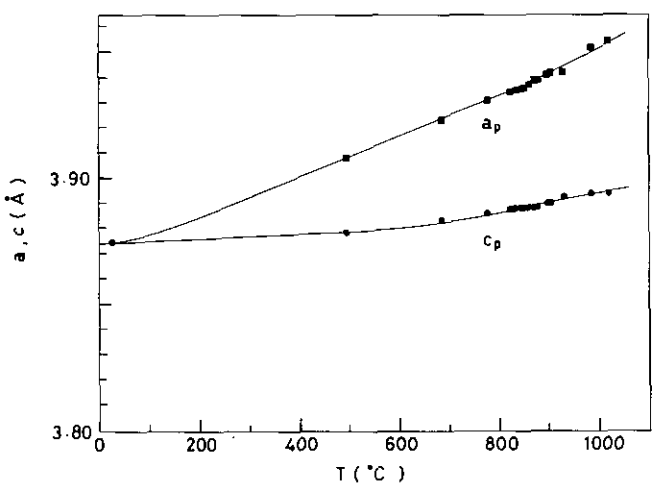

FIG. 5. Temperature dependence of lattice parameters of tetragonal $La_4BaCu_5O_y$ measured in air. The observed parameters, a_p and c_p are the fundamental perovskite parameters which are obtained by using Eq. (1).

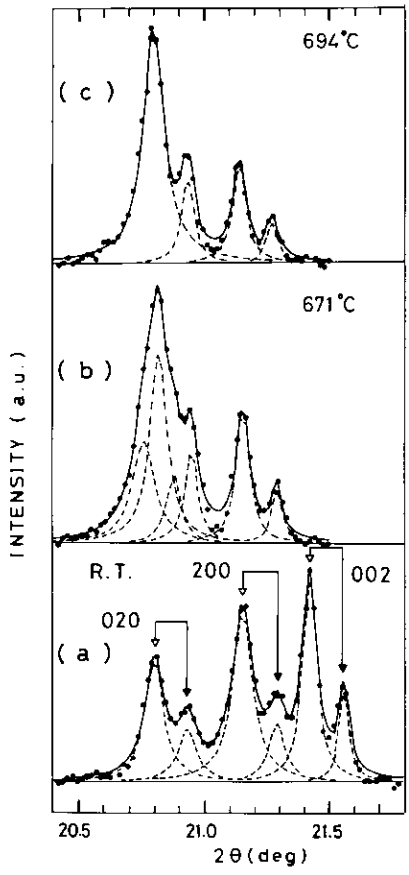

FIG. 6. HXRD patterns of monoclinic $La_4BaCu_5O_{12.5}$ in an evacuated quartz tube at (a) room temperature, (b) 671°C, and (c) 694°C. The Miller indices are based on the fundamental perovskite unit cell which are related to the monoclinic unit vectors by Eq. (2). Note that Mo$K\alpha$ radiation was used.

gens. For the monoclinic phase, as seen in Fig. 7, all the fundamental perovskite parameters a_p, b_p, and c_p, which are related to the monoclinic parameters by Eq. (2), increase linearly with temperature up to about 600°C. Assuming that the oxygen content y of the monoclinic phase is constant in the evacuated tube, we can consider this linear increase of the lattice parameter to be result of the thermal expansion. For the tetragonal phase, as seen in Fig. 5, a_p also increases at about the same rate as the lattice parameters of the monoclinic phase, although the increasing rate of c_p is less than $\frac{1}{5}$ that of a_p even above 800°C. Hence, it can be argued that the behavior of c_p of the tetragonal phase is caused by the influence of removed oxygens. Davies and Katzan (*8*) reported that c_p also contracted as the reduction proceeded. They considered that this contraction of c_p was caused by the change of the coordination of the CuO_6 octahedra. Based on this assumption, they proposed structural models for oxygen-deficient phases with $y = 12.5$, 12, and 11 in which oxygen vacancies are located in sites of the octahedra; for details of these models, see Ref. (*8*). Without direct experimental data, however, it is difficult to elucidate the site for removed oxygens and the crystal structure of the monoclinic phase.

We show DC resistivity data of tetragonal and monoclinic $La_4BaCu_5O_y$ in Fig. 11. The monoclinic $La_4BaCu_5O_{12.5}$, as well as the tetragonal one, is found to be a nonsuperconductor but a metallic conductor down to 2.6 K, although the residual resistivity of the monoclinic phase is much larger than that of tetragonal one. As a result, it might be concluded that the crystal structure of the monoclinic $La_4BaCu_5O_{12.5}$ does not include CuO_2 planes but still has a 3D Cu–O network.

4. Concluding Remarks

We have succeeded in synthesizing a new single-phase of monoclinic $La_4BaCu_5O_y$ by the reduction treatment in flowing N_2 gas at 780°C followed by slow cooling. At room temperature, the oxygen content y of the tetragonal $La_4BaCu_5O_y$ is found to be about 13.0 by the carbon reduction method and TGA in flowing H_2 gas, and the value of y of the monoclinic phase is determined to be 12.5 by TGA experiments. This new monoclinic phase has a unit cell of $\sqrt{10}a_p \times \sqrt{10}a_p \times a_p$, while the original tetragonal phase has a unit cell of $\sqrt{5}a_p \times \sqrt{5}a_p \times$

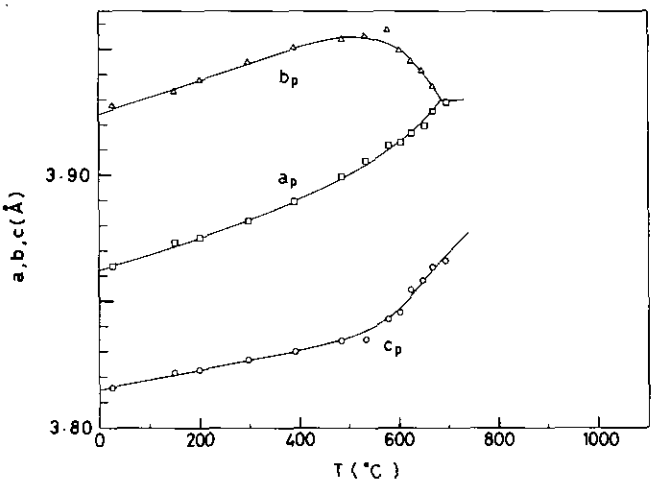

FIG. 7. Temperature dependence of lattice parameters of monoclinic $La_4BaCu_5O_{12.5}$ in an evacuated quartz tube. The observed parameters, a_p, b_p, and c_p, are the fundamental perovskite parameters which are obtained by using Eq. (2).

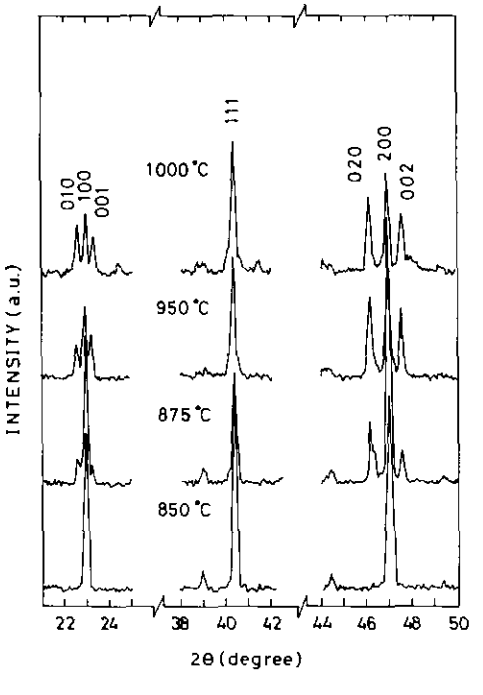

FIG. 8. XRD patterns for $La_4BaCu_5O_y$ compounds quenched into liquid N_2 after firing in air at various temperatures.

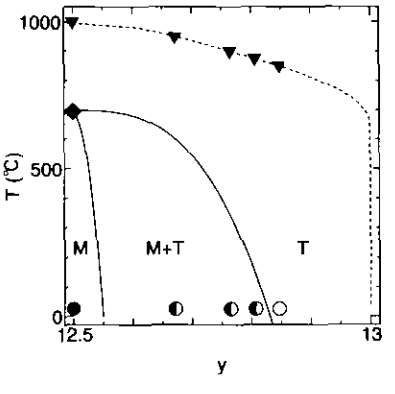

FIG. 9. A tentative phase diagram of $La_4BaCu_5O_y$ described as functions of oxygen content and temperature. The dashed line shows the temperature dependence of oxygen content in air obtained by TGA. Solid triangles (▲) show temperatures from which samples were quenched into liquid N_2. The obtained phases by quenching are described by following marks: (●) a single phase of monoclinic $La_4BaCu_5O_y$; (○) a single phase of tetragonal $La_4BaCu_5O_y$; and (◐) coexistence of monoclinic and tetragonal phases. A solid square (■) indicates the phase transition temperature in the evacuated tube. Solid curves represent expected boundary lines.

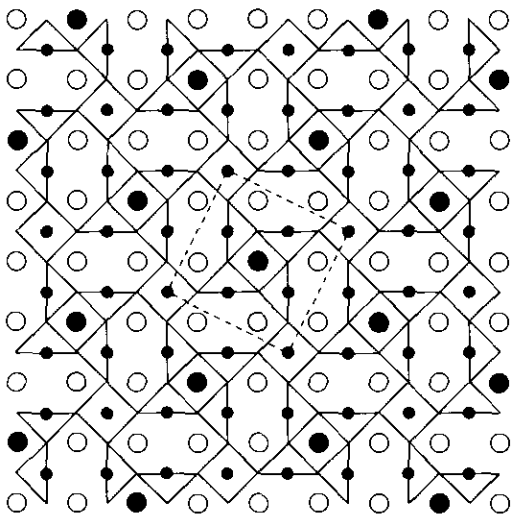

FIG. 10. A structural model by Michel *et al.* (*4*) for tetragonal $La_4BaCu_5O_{13.0}$ projected on the a–b plane. Open circles (○), large solid circles (●), and small solid circles (•) represent La^{3+}, Ba^{2+}, and Cu^{2+} ions, respectively. Ba^{2+} ions are located at $z = 0$ and the other cations take positions at $z = 0.5$. Oxygen ions at $z = 0$ are at the corners of triangles and squares. The other O^{2-} ions of $z = 0.5$ are located at the upper and lower sites of Cu^{2+} ions (apical sites).

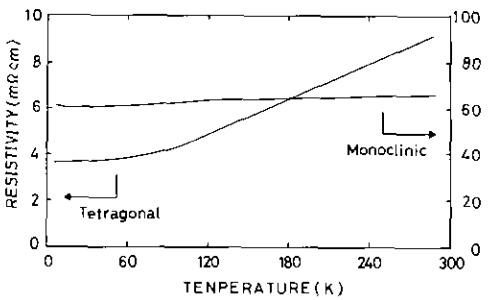

FIG. 11. Temperature dependence of the DC resistivities of tetragonal and monoclinic $La_4BaCu_5O_y$.

a_p. By means of TGA, it is revealed that y decreases from 13.0 to about 12.5 with increasing temperature in air. HXRD experiments show, however, that the unit cell has a tetragonal structure ($\sqrt{5}a_p \times \sqrt{5}a_p \times a_p$) independent of the temperature. On the other hand, the monoclinic $La_4BaCu_5O_y$ closed in an evacuated capillary tube is transformed to tetragonal above 670°C. This monoclinic phase is found to be a metallic conductor down to 2.6 K as is the tetragonal one.

Acknowledgments

The authors thank Mr. Y. Tsuchiya for his help with some parts of the HXRD experiment. They are grateful to Dr. K. Ban (Horiba Ltd.) for oxygen analysis. This work was supported by a Grant-in-Aid for Scientific Research on Priority Areas "Chemistry of New Superconductors" (01645004 and 02227102) from the Ministry of Education, Science, and Culture of Japan.

References

1. J. G. BEDNORZ AND K. A. MULLER, *Z. Phys. B* **64,** 189 (1986).
2. R. J. H. VOORHOEVE, "Advanced Materials in Catalysis," p. 129, Academic Press, New York (1977).
3. C. MICHEL, L. ER-RAKHO, AND B. RAVEAU, *Mater. Res. Bull.* **20,** 667 (1985).
4. C. MICHEL, L. ER-RAKHO, M. HERVIEU, J. PANNETIER, AND B. RAVEAU, *J. Solid State Chem.* **68,** 143 (1987).
5. J. B. TORRANCE, Y. TOKURA, A. NAZZAL, AND S. S. P. PARKIN, *Phys. Rev. Lett.* **60,** 542 (1988).
6. T. IMAI, H. YASUOKA, T. SHIMIZU, Y. UEDA, AND K. KOSUGE, *J. Phys. Soc. Jpn.* **58,** 1528 (1989).
7. N. KOJIMA, M. KATO, K. YOSHIMURA, K. KOSUGE, Y. UEDA, AND H. YASUOKA, *J. Jpn. Soc. Powder Powder Met.* **37,** 162 (1990).
8. P. K. DAVIES AND C. M. KATZAN, *J. Solid State Chem.* **88,** 368 (1990).